Neutrino-induced single pion production and the reanalyzed bubble chamber data

D. F. Tamayo Agudelo,[1] A. Mariano,[2,3] and D. E. Jaramillo Arango[1]

[1]*Facultad de C. Exactas y Naturales Universidad de Antioquia, Instituto de Física, Ciudad Universitaria: Calle 67 No 53-108 Bloque 6 Oficina 105, Medellin, Colombia*

[2]*Facultad de Ciencias Exactas Universidad Nacional de La Plata, C.C. 67,1900 La Plata, Argentina*

[3]*Instituto de Física La Plata CONICET, diagonal 113 y 63, 1900 La Plata, Argentina*

(Received 7 April 2022; accepted 7 June 2022; published 2 August 2022)

In this work we report the calculation of the charged current total and differential cross sections for weak pion production with neutrinos and antineutrinos, with the final pion-nucleon pair invariant mass $W_{\pi N} \lesssim 2$ GeV. Our results are compared with the recent reanalyzed data from the old bubble chamber experiments, that solved the discrepancy between the Argonne National Laboratory and Brookhaven National Laboratory data. We implement a model previously tested for the cuts $W_{\pi N} < 1.4$, 1.6 GeV, which explicitly includes resonances in the first and second resonance regions within different approaches for the resonances self-energy and $\frac{3}{2}$ vertexes and propagators, a fact not usually analyzed. Our model leans on consistently effective Lagrangians that generate resonant amplitudes together with nonresonant and resonant backgrounds. Effects of hadrons' finite extension and more energetic resonances correspond to the emitted pion-nucleon invariant mass in the $1.6 < W_{\pi N} < 2$ GeV region are taking into account using appropriate form factors in consistency with previous results on neutral current pion production calculations. Our results reproduce well the reanalyzed data without cuts and are compared with other models.

DOI: 10.1103/PhysRevD.106.033002

I. INTRODUCTION

For current and future neutrino oscillation experiments we need to understand single pion production by neutrinos with few-GeV energies. The pion production is either a signal process when scattering cross sections are analyzed, or a large background for analyses which select quasielastic events. At these energies the dominant production mechanism is via the excitation and subsequent decay of hadronic resonances. Experimental data on nuclear targets present a confusing picture, shown from the MINERνA [1,2] and MiniBooNE [3] experiments in poor agreement with each other in the framework of current theoretical models [4,5]. Complete models of neutrino nucleus single pion production interactions are usually factorized into three parts: the neutrino-nucleon cross section; additional nuclear effects which affect the initial interaction; and the "final state interactions" (FSI) of hadrons exiting the nucleus.

More basically at the level of a neutrino-nucleon cross section, the axial form factor (FF) for pion production on free nucleons cannot be constrained by electron scattering data, used normally to get the vector FF, so it relies upon data from Argonne National Laboratory's 12 ft bubble chamber (ANL) [6] and Brookhaven National Laboratory's 7 ft bubble chamber (BNL) [7]. The ANL neutrino beam was produced by focusing 12.4 GeV protons onto a beryllium target. Two magnetic horns were used to focus the positive pions produced by the primary beam in the direction of the bubble chamber, these secondary particles decayed to produce a predominantly ν_μ peaked at ~0.5 GeV. The BNL neutrino beam was produced by focusing 29 GeV protons on a sapphire target with a similar two horn design to focus the secondary particles. The BNL ν_μ beam had a higher peak energy of ~1.2 GeV and was broader than the ANL one. These both datasets differed in normalization by 30–40% for the leading pion production process $\nu_\mu p \to \mu^- p \pi^+$, which resulted in large uncertainties in the predictions for oscillation experiments as well as in the interpretation of data taken on nuclear targets [8–13].

It has long been suspected that the discrepancy between ANL and BNL was due to an issue with the normalization of the flux prediction from one or both experiments, and it has been shown by other authors that their published results are consistent within the experimental uncertainties provided [14,15]. Reference [16] presented a method for removing flux normalization uncertainties from the ANL

and BNL $\nu_\mu p \to \mu^- p\pi^+$ measurements by taking ratios with charged-current quasielastic (CCQE) event rates in which the normalization cancels. Then, a measurement of $\nu_\mu p \to \mu^- p\pi^+$ was obtained by multiplying the ratio by an independent measurement of the charged-current quasielastic cross section, which is well known for nucleon targets. Using this technique, they found good agreement between the ANL and BNL $\nu_\mu p \to \mu^- p\pi^+$ datasets. Later, they extend that method to include the subdominant $\nu_\mu n \to \mu^- p\pi^0$ and $\nu_\mu n \to \mu^- n\pi^+$ channels [17]. These authors used the resulting data to fit the parameters of the GENIE pion production model [18]. They found a set of parameters that can describe the bubble chamber data better than the GENIE default ones, and provided updated central values and reduced uncertainties for use in neutrino oscillation and cross section analyses that use the GENIE model. In this model the cross section is cut off at a tunable invariant mass value, which is $W_{\pi N} \leq 1.7$ GeV by default. No in-medium modifications to resonances are considered, and interferences between resonances are neglected in the calculation being the Rein-Sehgal (RS) model in Ref. [19] adopted. Nevertheless, the original RS model includes nonresonant single pion production as an additional resonance amplitude, while in GENIE the nonresonant component is implemented as an extension of the deep inelastic scattering model. They found that GENIE's nonresonant background prediction has to be significantly reduced to fit the data, which may help to explain the recent discrepancies between simulation and data observed by the MINERνA coherent pion and NOνA [20] oscillation analyses. While more sophisticated single pion production models exist, the GENIE generator is widely used by current and planned neutrino oscillation experiments, so tuning the generator parameters represents a pragmatic approach to improving its description of available data. We find that the reanalyzed data, where the normalization discrepancy has been resolved, is able to significantly reduce the uncertainties on the pion production parameters.

This is one of the reasons why we are encouraged to return to the calculation of neutrino-nucleon cross sections in our model and try to extend it to larger final $W_{\pi N}$ invariant masses. On the other hand, there are many models to describe this process that do not fulfill several important ingredients:

(1) There are problems from the formal point of view. The main pion emission source are excitation and decay of resonances, and many of them are of spin $\frac{3}{2}$ where its field is built as $\Psi_\mu \equiv \psi \otimes \xi_\mu$, where ψ is a Dirac spinor field and ξ_μ is a Dirac four-vector [21]. In this way, the field Ψ_μ will contain a physical spin-$\frac{3}{2}$ sector and a spurious spin-$\frac{1}{2}$ sector dragged by construction. Nevertheless, involved Lagrangians must lead to amplitudes invariant by contact transformations [22] $\Psi^\nu \to \Psi'^\nu = R_{\mu\nu}(\frac{1+3A}{2})\Psi^\nu$, $R^{\rho\sigma}(a) = g^{\rho\sigma} + a\gamma^\rho\gamma^\sigma$, which change the amount of the spin-$\frac{1}{2}$ espurious contribution since there exist the constraint $\Psi_\mu\gamma^\mu = 0$ for the $\frac{3}{2}$ sector. Many works keep the simpler forms of both the free and interaction Lagrangians involving Ψ_μ that correspond to different A values, and with this choice amplitudes lacks the mentioned invariance. In addition, the interaction Lagrangian for the spin-$\frac{3}{2}$ field coupled to a nucleon N (ψ) and a pseudoscalar meson (ϕ) or boson (W), as usually appears in a resonance production decay, depends on a second parameter Z not fixed by the contact invariance. Now to fix it, we point to the question of the true degree of freedom of the spin-$\frac{3}{2}$ field; where the dynamics is described by a constrained quantum field theory. Observe that in the free Ψ_μ Lagrangian there is no term containing $\dot{\Psi}_0$ [23]. So, the equation of motion for it is a true constraint, and Ψ_0 should have no dynamics. It is necessary then that interactions do not change that fact, and as was shown in Ref. [23] this is fulfilled for certain values of Z. These formal points are usually not analyzed in the majority of works on the field.

(2) In addition to the resonances pole or direct contribution (normally referred to as direct resonant or simply resonant terms) to the amplitude, we have background terms coming from cross resonance amplitudes (usually named the background resonant terms) and nonresonance origin (usually called the background nonresonant terms). Many works do not consider the interference between these both resonant and background contributions, and really it is very important to describe the data.

(3) Finally, other models detach the decay process from the resonance production out of the whole weak production amplitude. However, resonances are nonperturbative phenomena associated to the pole of the S-matrix amplitude and one cannot detach them from its production or decay mechanisms. Further, the models to describe cross sections use born contributions for the background amplitudes and resonant ones that are valid around each resonance region. Nevertheless, the effect of deviations from the hadronic pointlike couplings due to the quark structure of nucleons and resonances are not taken into account when the final πN invariant mass $W_{\pi N}$ grows, and it is assumed that the models are valid for all $W_{\pi N}$ regions.

In this work we calculate the total and differential cross sections of the inelastic dispersion of neutrinos on nucleons with the production of one pion until $W_{\pi N} \lesssim 2$ GeV and we try to describe the reanalyzed data in Refs. [16,17]. In our model we incorporate explicitly resonance states $\Delta(1232)$, and $N^*(1440)$, $N^*(1520)$, $N^*(1535)$, the so-called second resonance region, with a consistent model for the spin-$\frac{3}{2}$ fields that reproduced satisfactorily the data for the ANL experiment in the range $W_{\pi N} \lesssim 1.6$ GeV [24]. The effect of hadron structure when $W_{\pi N}$ grows and of more energetic resonances, not introduced explicitly in the model, is included throughout a global effective hadronic FF in consistence with previous

calculations for neutral currents (NCs) [25]. Our model reproduces well the data of Refs. [16,17], both for the total and differential cross sections.

Our work will be organized as follows: In Sec. II, we summarize the general description of the pion production cross sections, together with the previously calculated amplitudes showed in the Appendix. In Sec. III we analyze how to extend our previous model to higher $W_{\pi N}$ and will show our results for neutrino and antineutrino scattering. Finally, in Sec. IV, we summarize our conclusions.

II. TOTAL AND DIFFERENTIAL CROSS SECTIONS

We resume here some general concepts and let specific formulae for an Appendix. We are interested in describing here two observables for the CC $\nu N \to \mu^+ N'\pi$ and $\bar{\nu}N \to \mu^- N'\pi$ modes, since NC processes in the present $W_{\pi N}$ range, where analyzed previously [25]. The total cross section for single pion weak production on nucleons, where we use νN center mass (CM) variables since it is easier to look for their limits, reads (we take $\boldsymbol{p}_\nu = E_\nu \hat{\boldsymbol{k}}$ along the z axis)

$$\sigma(E_\nu^{\rm CM}) = \frac{m_\nu m_N^2}{(2\pi)^4 E_\nu^{\rm CM}\sqrt{s}} \int_{E_\mu^-}^{E_\mu^+} dE_\mu^{\rm CM} \int_{E_\pi^-}^{E_\pi^+} dE_\pi^{\rm CM} \times \int_{-1}^{+1} d\cos\theta \int_0^{2\pi} d\eta \frac{1}{16} \sum_{\rm spin} |\mathcal{M}|^2, \tag{1}$$

being $\sqrt{s} = E_\nu^{\rm CM} + E_N^{\rm CM} = \sqrt{2E_\nu m_N + m_N^2}$, $d\Omega_\mu = d\cos\theta d\phi$ and $d\Omega_\pi = d\cos\xi d\eta$, and where $d\phi$ and $\cos\xi$ integrations are not present due to symmetry and conservation fixing, respectively. The limits $E_\mu^\pm$ and $E_\pi^\pm$ can be found trivially from momentum conservation (see Ref. [26]), and where the connection with neutrino's energy in LAB is given by

$$E_\nu^{\rm CM} = \frac{m_N E_\nu}{\sqrt{2E_\nu m_N + m_N^2}}, \tag{2}$$

being the LAB four momenta involved in Eqs. (1) and (2) defined as

$$p_\nu = (E_\nu, \mathbf{p}_\nu), \quad p_\mu = (E_\mu, \mathbf{p}_\mu), \quad \mathrm{k} = (E_\pi, \mathbf{k}), \quad p = (E_N, \mathbf{p}), \quad p' = (E_{N'}, \mathbf{p}'),$$

with $E(\boldsymbol{\xi}) = \sqrt{|\boldsymbol{\xi}|^2 + m^2}$ (we set $m_\nu = 0$), with the same expressions and definitions for $\bar{\nu}$. On the other hand, since it is the tool for fixing axial resonance parameters by comparison with the ANL and BNL data experiments [6,7] of the neutrino flux averaged cross section, we will calculate the flux averaged differential cross section defined as ($Q^2 = -(p_\mu - p_\nu)^2$)

$$\left\langle \frac{d\sigma}{dQ^2} \right\rangle = \frac{\int_{E_\nu^{\rm min}}^{E_\nu^{\rm max}} \frac{d\sigma(E_\nu)}{dQ^2} \phi(E_\nu) dE_\nu}{\int_{E_\nu^{\rm min}}^{E_\nu^{\rm max}} \phi(E_\nu) dE_\nu}, \tag{3}$$

with $\phi(E_\nu)$ being the neutrino's flux. The total amplitude $\mathcal{M}$ for the considered process reads

$$\mathcal{M} = i\frac{G_F^2}{\sqrt{2}} \bar{u}(p_\mu)(-)i\gamma^\lambda(1-\gamma_5)u(p_\nu) i g_{\lambda\lambda'} V_{ud} \bar{u}(p') \times \mathcal{O}^{\lambda'}(p', k, p, q)u(p), \tag{4}$$

with the spin and isospin indexes being omitted, $G_F = 1.16637 \times 10^{-5}$ GeV^{-2}, $|V_{ud}| = 0.9740$, and $\mathcal{O}^{\lambda'}$ is the vertex generated by the hadronic CC current; this is present in the weak interaction Lagrangian and the strong vertexes and hadron propagators (see Refs. [25,26]). $\bar{u}O^\lambda u$ includes the $WN \to \mu N'\pi$ processes present in Fig. 1 and defines the contribution of a Feynman graphs to a channel; the results are the isospin coefficients shown below.

We can split $\mathcal{O}^\lambda$ as

$$\mathcal{O}^\lambda = \mathcal{O}^\lambda{}_{\rm B} + \mathcal{O}^\lambda_{\rm R}, \tag{5}$$

where $\mathcal{O}_{B,R}$ generate the tree-level hadronic amplitudes contributing to the background (B), nucleon Born terms

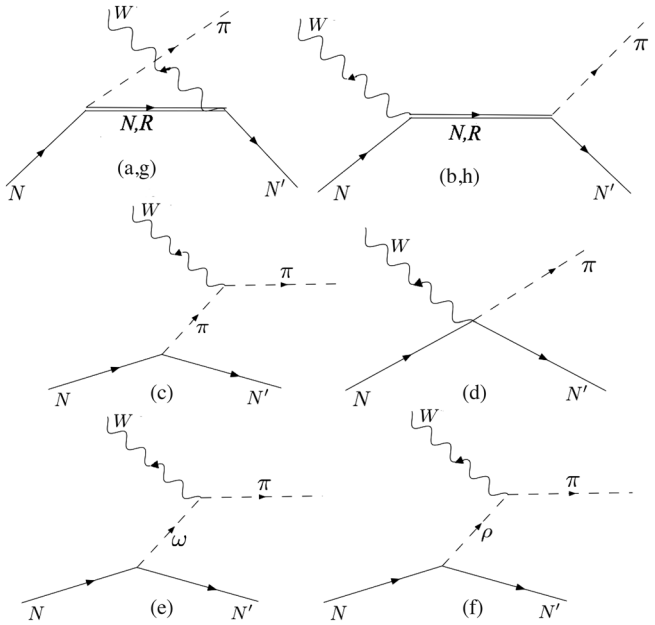

FIG. 1. Terms in the scattering amplitude for the process $\nu(\bar{\nu})N \to \mu N'\pi$. We indicate with (a) the first graph with a nucleon (N) as intermediate state and with (h) when the intermediate state is a resonance (R), since we have the same topological form. The same is true for the second graph where we use (b) and (g) for the N and R intermediate contributions respectively. Terms (a)–(g) represent the background (B) contribution. Term (h) is a the direct or pole resonant contribution (R).

[Figs. 1(a) and 1(b)], the meson exchange amplitudes (contact term included) [Figs. 1(c)–1(f)], and the resonance-crossed term [Fig. 1(g)]. The direct or pole resonant contribution (R) is shown in Fig. 1(h), and it is necessary that the resonance acquires a width in order to avoid the singularity in the propagator by a self-energy dressing that can be treated within different approximations. The effect of the self energy could, in principle, change the full structure of the propagator. In the case of spin-$\frac{1}{2}$ resonances, the unstable character introduced by this self-energy accounts for the replacement

$$m_R \to m_R - i\frac{\Gamma_R(s)}{2} \tag{6}$$

into the unperturbed propagator without changing its structure. This width Γ_R is obtained by considering the pion-nucleon loop contribution to the self-energy [9] and reads

$$\begin{aligned}\Gamma_R(s)\times B_r &= \frac{3}{4\pi}\left(\frac{f_{\pi NR}}{m_\pi}\right)^2 (m_R+\pi m_N)^2 \\ &\times \left(\frac{(\sqrt{s}-\pi m_N)^2-m_\pi^2}{4s^{3/2}}\right)\lambda^{\frac{1}{2}}(s,m_N^2,m_\pi^2), \\ \lambda(x,y,z) &= x^2+y^2+z^2-2xy-2xz-2yz,\end{aligned} \tag{7}$$

with $\pi=\pm$ being the parity, B_r the corresponding πN branching ratio decay, and $f_{\pi NR}$ the strong coupling.

For the spin-$\frac{3}{2}$ resonances the inclusion of the pion-nucleon loop in the self energy alters the full structure of the propagator due to the presence of spurious $\frac{1}{2}$ components. Nevertheless, if we neglect terms of order $(f_{\pi NR}/m_\pi)^4$ and $((m_R-\sqrt{s})(f_{\pi NR}/m_\pi)^2)$ (see Ref. [27]), which are expected to be very small in the resonance region $(\sqrt{s}\approx m_R)$, we keep the unperturbed form with the same replacement (6) and now

$$\begin{aligned}\Gamma_R(s)\times B_r &= \frac{\mathcal{I}_R\left(\frac{f_{\pi NR}}{m_\pi}\right)^2}{4\pi}\left(\frac{(\sqrt{s}+\pi\times m_N)^2-m_\pi^2}{48s^{5/2}}\right) \\ &\times \lambda^{\frac{3}{2}}(s,m_N^2,m_\pi^2),\end{aligned} \tag{8}$$

where $\mathcal{I}_R=\{^1_3$ for $I=\{^{\frac{1}{2}}_{\frac{3}{2}}$, respectively.

If one analyzes the formal scattering T-matrix theory [28] for the final πN pair in both elastic scattering or pion photoproduction, then it is mandatory that the πNR vertex should be also dressed as the propagator by the πN rescattering through nonpole amplitudes. This makes also the vertex s dependent, or in other words we get an effective coupling constant $\frac{f_{\pi NR}(s)}{m_\pi}$ due to the decay [28] mediated by the intermediate πN propagator (this will be analyzed deeply below). In previous works, the approach resulting from the formal limit of massless N and π in the loop contribution to the Δ self-energy and in the dressed $\pi N\Delta$ vertex has been considered. This was called the complex-mass scheme (CMS) [29]. In this formal limit the vertex dressing gives a dependence $f_{\pi N\Delta}(s)=\frac{\kappa f^0_{\pi N\Delta}}{\sqrt{s}}$, with $f^0_{\pi N\Delta}$ being the bare $\pi N\Delta$ coupling constant and κ a constant of dimension MeV to fit, in place of doing the complex calculation of the integral involved in the vertex correction. Within the CMS we derive from (8) the approximated expression ($B_r\approx 1$ for the Δ)

$$\Gamma_\Delta(s)=\left(1-\frac{\sqrt{s}-m_R}{m_R}\right)\Gamma_\Delta^{\rm CMS},\quad \Gamma_\Delta^{\rm CMS}=\frac{\kappa^2\left(\frac{f^0_{\pi NR}}{m_\pi}\right)^2}{192\pi}m_\Delta. \tag{9}$$

When $s\simeq m_\Delta^2$ we get a constant width $\Gamma_\Delta(s)\approx\Gamma_\Delta^{\rm CMS}$, where $\Gamma_\Delta^{\rm CMS}$ is fitted in place of κ together $\frac{f_{\pi N\Delta}}{m_\pi}$ and m_Δ to reproduce π^+p scattering [30]. Another approach commonly used [9], is to fix $\sqrt{s}\approx m_\Delta$ in (7) or (8) and to use the experimental values for m_Δ and Γ_Δ times B_r, and get $f_{\pi NR}$. We will refer to this as a constant mass-width approach (CMW). We will use both the CMS and CMW depending on the considered resonance.

The explicit expressions for $\mathcal{O}_B$, split in those coming from the nucleon and meson exchange contributions in Figs. 1(a)–1(f) (BN) and from the resonances in Fig. 1(g) (BR), and $\mathcal{O}_R$ for $R\equiv\Delta(1232)$, $N^*(1440)$, $N^*(1520)$, $N^*(1535)$ are shown in the Appendix. These are obtained in Ref. [24]. We only show here the isospin factors for each contribution to the amplitude (see Fig. 1) since it will be useful for the results section. They are indicated with $\mathcal{T}(m_t\equiv p,n,n,m_{t'}\equiv p,p,n)$ (or charge conjugate for $\bar{\nu}$) and can be obtained using the isospin operators present in the interaction Lagrangians together with the isospin wave functions for the W boson and the hadrons (see Refs. [25,26])

$$\begin{aligned}\mathcal{T}_a &= \mathcal{T}_g^{1440,1535,1520} = -2,0,-\sqrt{2}, \\ \mathcal{T}_b &= \mathcal{T}_h^{1440,1535,1520} = 0,-2,\sqrt{2}, \\ \mathcal{T}_c &= 1,-1,\sqrt{2}, \\ \mathcal{T}_d &= -1,1,-\sqrt{2}, \\ \mathcal{T}_e &= -1,-1,0, \\ \mathcal{T}_f &= 1,1,-\sqrt{2}, \\ \mathcal{T}_g^\Delta &= -1/3,-1,\sqrt{2}/3, \\ \mathcal{T}_h^\Delta &= -1,-1/3,-\sqrt{2}/3.\end{aligned} \tag{10}$$

III. EXTENSION TO HIGHER $W_{\pi N}$ AND RESULTS

In this work we analyze the total and differential cross sections for the CC modes of the six processes

$$\begin{aligned} &\nu p \to \mu^- p\pi^+, \qquad \nu n \to \mu^- p\pi^0, \qquad \nu n \to \mu^- n\pi^+, \\ &\bar{\nu} n \to \mu^+ n\pi^-, \qquad \bar{\nu} p \to \mu^+ n\pi^0, \qquad \bar{\nu} p \to \mu^+ p\pi^-, \end{aligned} \tag{11}$$

with neutrino energies exciting the $W_{\pi N} = \sqrt{(p'+k)^2} \leq 2$ GeV region. We will obtain these cross sections through the Eqs. (1)–(3) with the amplitude (4), taking $(1+\gamma_5)$ when $\nu \to \bar{\nu}$, and the vertex production contributions in Eqs. (A1)–(A3) of the Appendix. We have included explicitly the resonances of the first and second region $(\Delta(1232), N^*(1440), N^*(1520), N^*(1535))$, while the effect of more energetic ones will be included indirectly. A calculation with the cuttoff $W_{\pi N} \lesssim 1.6$ GeV using the above mentioned CMS approach for the $\Delta(1232)$ and CMW for the other resonances, described properly σ, $\frac{d\sigma}{dQ^2}$, $\frac{d\sigma}{dW_{\pi N}}$ [24] for the ANL data. We have treated in consistent fashion the spin-$\frac{3}{2}$ resonances from the point of view of contact invariance and the true considered degree of freedom of the spin-$\frac{3}{2}$ field, both points mentioned in the Introduction, choosing the values $A = -\frac{1}{3}$, $Z = \frac{1}{2}$. Now, we wish to extend our model to higher energies in order to describe the data of the recent reanalyzed ANL and BNL data without cuts [17]. On going to higher energies we can ask ourselves two important questions. First, is it possible to pursue the tree level model used for the background or the CMS and CMW approaches to treat the resonances for any energy $W_{\pi N}$ with pointlike hadrons? Second, is it enough simply to add more and more resonances to describe the $W_{\pi N} > 1.6$ GeV region? We will intend to analyze these questions within the frame of πN rescattering, not considered in detail until now, in the following subsections.

A. Rescattering and hadrons FF

We support our discussion on the pion photoproduction reaction analyzed in Ref. [28], and we have the analogy $\mathcal{O}^\lambda \equiv \hat{B}^\lambda$ and $\mathcal{O}^\lambda_{B,R} \equiv \hat{B}^\lambda_{NP}, \hat{B}^\lambda_P$ with the photoproduction vertexes in that reference. The approximation implemented previously until the second resonance region [24] can be resummed as

$$\mathcal{O}^\lambda \approx \mathcal{O}^\lambda_B + \mathcal{O}^\lambda_R \equiv \mathcal{O}^\lambda_B + \sum_R V_{R\pi N} G_R W^\lambda_{WNR}, \tag{12}$$

where $V_{R\pi N}$ and W^λ_{WNR} represent schematically the $R \to N\pi$ and $WN \to R$ vertexes, respectively, while G_R is a resonance propagator. Nevertheless, the $\mathcal{O}^\lambda_B$ contributions, in particular the $\mathcal{O}^\lambda_{\mathrm{BR}}$ coming from the $\frac{3}{2}$ resonances [Fig. 1(g)], cannot be dressed by the self-energy, which is not affected by a πN rescattering in (12) as is done in $\mathcal{O}^\lambda_R$ with Γ_R. As a consequence, its contribution to the amplitude grows rapidly for $W_{\pi N} \gtrsim 1.5$ GeV as will be shown below. As described in Ref. [28] for the case of photoproduction, but which is also valid here, there are other effects not considered. The complete excitation amplitude in the final πN CM is

$$\mathcal{O}^\lambda(k,q) = [-i(2\pi)^4\delta^4(k-k') + T_{NP}(k')G_{\pi N}(k')]\left(\mathcal{O}^\lambda_B(k',q) + \sum_R V_{R\pi N}(k',k)G_R(k)\tilde{W}^\lambda_{WNR}(k,q)\right), \tag{13}$$

$$\tilde{W}^\lambda_{WNR}(k,q) = W^\lambda_{WNR}(k,q) + (V_{R\pi N}(k,k'') + V_{R\pi N}(k,k')G_{\pi N}(k')T_{NP}(k',k''))G_{\pi N}(k'')\mathcal{O}^\lambda_B(k'',q), \tag{14}$$

where k', k'' are intermediate pion momenta and a repeated k, k', k'' indicate $i\frac{\int dk,k',k''^4}{(2\pi)^4}$, and

$$G_{\pi N}(k') = S_N(p+q-k')\Delta_\pi(k'),$$

is the pion-nucleon intermediate propagator and T_{NP} is the nonpole scattering T matrix that iterates to all orders the potential $V_{NP} \equiv V_{N\pi,N'\pi'}$ built with nucleon Born terms, meson exchange t contributions and u-resonant contributions. In summary, in the full amplitude the rescattering of the final πN pair through T_{NP} is considered as well the decay into a resonance of $\mathcal{O}^\lambda_B$. We will not introduce in this work unitarizartion corrections, done through imaginary contributions in (13), since as we are analyzing the total and differential cross sections, where corrections to each multipole compensate out in the multipole expansion of the cross section [28]. As we wish to deal with effective real coupling constants (T_{NP} dresses but is a complex operator), it is convenient to express the πN T-matrix operator in terms of the real K matrix [28], and after a three-dimensional reduction we get [28]

$$\mathcal{O}^{\lambda}(\boldsymbol{k},\boldsymbol{q},W_{\pi N}) \approx [(2\pi)^3\delta^3(\boldsymbol{k}-\boldsymbol{k}') + \mathcal{P}(K_{NP}(\boldsymbol{k},\boldsymbol{k}')G_{TH}(\boldsymbol{k}',\sqrt{s})], \times \left[\mathcal{O}^{\lambda}_{B}(\boldsymbol{k}',\boldsymbol{q},W_{\pi N})) + \sum_{R} V_{R\pi N}(\boldsymbol{k}',\boldsymbol{p}))G_{R}(\boldsymbol{p},W_{\pi N})\tilde{W}^{\lambda}_{WNR}(\boldsymbol{p},\boldsymbol{q},W_{\pi N})\right], \tag{15}$$

$$\tilde{W}^{\lambda}_{WNR}(\boldsymbol{p},\boldsymbol{q},W_{\pi N}) = W^{\lambda}_{WNR}(\boldsymbol{p},\boldsymbol{q}) + \mathcal{P}[V_{R\pi N}(\boldsymbol{p},\boldsymbol{k}')G_{TH}(\boldsymbol{k}',W_{\pi N})\mathcal{O}^{\lambda}_{B}(\boldsymbol{k}',\boldsymbol{q})], \tag{16}$$

where $G_{\pi N}(k')$ is replaced by the Thompson propagator $G_{TH}(\boldsymbol{k}',W_{\pi N}) = \frac{m_N}{2E_\pi(\boldsymbol{k}')E_N(\boldsymbol{k}')}\sum_{ms'}\frac{u(-\boldsymbol{k}',m_s')\bar{u}(\boldsymbol{k}',m_s')}{W_{\pi N}-E_\pi(\boldsymbol{k}')-E_N(\boldsymbol{k}')}$ and where $\mathcal{P}$ is the principal value on the integral in repeated momenta.

In order to reproduce the experimental data FF have to be introduced which affect both $\mathcal{O}^{\lambda}_{B,R}$ to regularize the integrals in (15) and (16). They are meant to model the deviations from the pointlike couplings due to the quark structure of nucleons and resonances, analogs of the electromagnetic ones reflecting the extension of the hadrons and should be calculated from the underlying theory or quark models [31]. Because it is not clear *a priori* which form these additional factors should have, they introduce a source of systematical error in all models [32]. Guided by an our previous proper description of NC1π data obtained by the CERN Gargamelle experiment without applying cuts in the neutrino energies [25], we multiply $\mathcal{O}^{\lambda}_{B}+\mathcal{O}^{\lambda}_{R}$ by a global regularizing FF of the $R\pi N$ and $N\pi N'$ vertexes ($\mathrm{k}=|\boldsymbol{k}|$)

$$F(\mathrm{k},W_{\pi N}) = \frac{(\Lambda)^4}{(\Lambda)^4+\mathrm{k}(\mathrm{W}_{\pi\mathrm{N}})^2(W_{\pi N}-W^{\mathrm{th}}_{\pi N})^2\theta(W_{\pi N}-1.6\ \mathrm{GeV})}, \tag{17}$$

$$\mathrm{k}(W_{\pi N}) = \sqrt{\frac{(W^2_{\pi N}-m^2_N-m^2_\pi)^2-4m^2_Nm^2_\pi}{4W^2_{\pi N}}}, \tag{18}$$

being the threshold invariant mass $W^{\mathrm{th}}_{\pi N}=m_\pi+m_N$, which is consistent with that introduced in Refs. [33,34] ([35]), but we light it above the second resonance region since it was shown that the description with the $W_{\pi N}\lesssim 1.6$ GeV was correct within our model [24]. This FF can be seen as

$$F(\mathrm{k},W_{\pi N}) = \frac{(\Lambda_{\mathrm{eff}})^2}{(\Lambda_{\mathrm{eff}})^2+\mathrm{k}(\mathrm{W}_{\pi\mathrm{N}})^2}, \quad \Lambda_{\mathrm{eff}} = \Lambda\frac{\Lambda}{W_{\pi N}-W^{\mathrm{th}}_{\pi N}}, \tag{19}$$

where we have a monopole FF with an effective cutoff diminishing with $W_{\pi N}-W^{\mathrm{th}}_{\pi N}$, making sure that that certain term "disappears" or contributes less in the amplitude since $W_{\pi N}$ grows another resonance, which is not considered in the amplitude, that could be excited. Note that this FF affects also the on shell contributions, i.e., the terms surviving in (15) when the $\mathcal{P}$ terms are dropped.

In conclusion, to get the full amplitudes in Eq. (15) we need to add the FF taking into account the hadron extensions since, as can be seen in $G_{TH}(\boldsymbol{k}',W_{\pi N})$, we keep the π and N elemental character for any $W_{\pi N}$, and this makes the involved integral divergent. This entails to moderate the on shell amplitude $\mathcal{O}^{\lambda}$ with this FF, which is not considered in the approach (12).

B. Results

We adopt the same model as in a recent work [24], where we have calculated the pion production cross section including explicitly spin-$\frac{1}{2}$ and -$\frac{3}{2}$ resonances $\Delta(1232)$, $N^*(1440)$, $N^*(1520)$, and $N^*(1535)$ in the calculus of the amplitudes (A1), (A2), and (A3) in the Appendix to cover the so-called second resonance region. The formal aspects mentioned in the introduction an related with the spin-$\frac{3}{2}$ Lagrangians (free and interaction) regards the contact-transformation parameter and the additional Z parameter present in the $\mathcal{L}_{\pi NR}$ interaction Lagrangian, have been discussed in that reference. The nonresonant contributions in (A1) are also described in [24] together all the adopted FF. We treat the spin-$\frac{1}{2}$ resonances within the parity conserving parametrization for the FFs, since this is compatible to that used in the similar topological nucleon contribution in Figs. 1(a) and 1(b). For the spin-$\frac{3}{2}$ resonances we use the Sachs parametrization to be consistent with our previous works including only the Δ resonance, where we get better results instead of using the parity conserving resonance [36]. We followed the connection between both parametrizations achieved in that reference to get the FF for the $N^*(1520)$ resonance, and have taken the Q^2-dependent FF from Ref. [37] for all the second region resonances. The main channel $\nu p\to\mu^-\pi^+p'$ with the cut $W_{\pi N'}<1.4$ GeV in the final invariant mass is used to fix the main axial Δ-coupling constant $D_1(0)$ [26,28]. With this cut it was shown [24], at less for this channel, that the contributions of more energetic resonances than the $\Delta(1232)$ are small and are important only for more energetic cuts. As the reanalyzed data of ANL achieved in Ref. [17] does not affect appreciably the channel used to fit $D_1(0)$ for $W_{\pi N'}<1.4$ GeV, then we will not make a new

fitting to $\langle \frac{d\sigma}{dQ^2} \rangle$. In our previous work [24] we achieved the comparison with the data of ANL experiment in the region of $W_{\pi N} < 1.4$, 1.6 GeV, where we have worked within the CMS + CMW approach. From the results including and not including the second resonance region, we concluded that to describe the data in all channels this resonance region should be included. We concluded that these resonances influence through their tails, since they have their centroids over these cuts. At the amplitude level, these tails interfere with the other resonances and background contributions. This behavior is confirmed when we compared the data with the $W_{\pi N} < 1.6$ GeV measurement and is in good agreement with the data for the antineutrino case.

Nevertheless, the ANL data of Ref. [6] contains results without energy cuts, and all results in Ref. [7] are reported without events exclusion. In addition, the reanalysis of these two sets of data has been done recently in Refs. [16,17], where the main results of the cross section are obtained with a tunable invariant mass value, which is $W \leq 1.7$ GeV compared with data without cuts. For describing them we need to extend our model to higher energies. The main questions seem to be these: Do we add more energetic resonances keeping the approach in Eq. (12)? Or do we put attention on the FF discussion in the previous subsection? In the Fig. 2 we show the total cross section (1) calculated with the amplitude (4) obtained

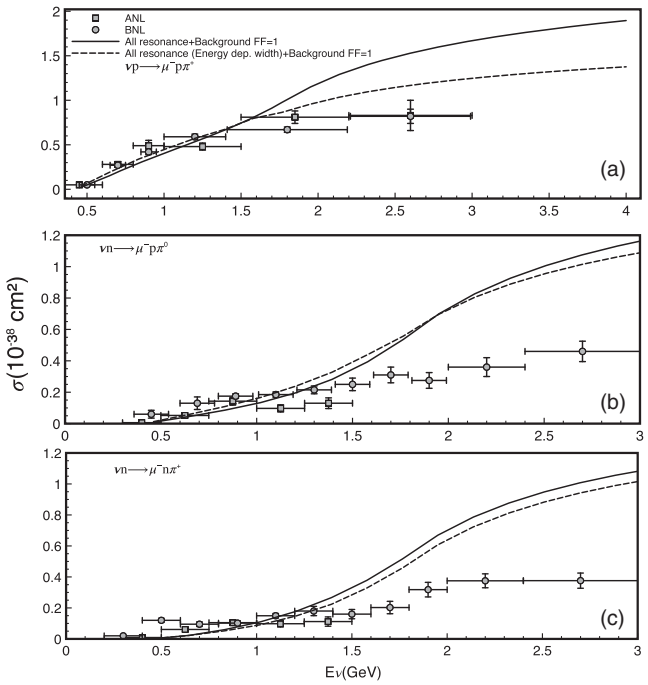

FIG. 2. Total νN cross section as a function of the neutrino energy for different channels and $F(\mathrm{k}, W_{\pi N}) = 1$. Results with Δ + second region resonances plus the corresponding background in each case are shown for a cut $W_{\pi N} \lesssim 2$ GeV with dotted and full lines. Results within CMS + CMW and with energy dependent width are shown with dashed lines. Data are taken from Ref. [6]

from the approach (12) and Eqs. (A1)–(A3) in the Appendix. Now we enable $W_{\pi N} \lesssim 2$ GeV, and, as can be seen, the cross section grows with a departure from the data. With full lines we show the results of the CMS + CMW approach for the resonances with a constant width, while with dashed lines we show results that used the same masses m_R and coupling constants $f_{\pi NR}$ but with energy dependent widths given by Eqs. (7) and (8). As can be seen with a better width's approach, which means a most exact treatment in the resonance self-energy, the description for the first channel improves appreciably. In it, the direct contribution [Fig. 1(h)] for the Δ, with $\mathcal{T}_h^{\Delta 2} = 1$ in Eq. (10), is the main contribution being the cross one with $\mathcal{T}_g^{\Delta 2} = 1/9$ being very small. For the other two channels, this contribution is much lower since $\mathcal{T}_h^{\Delta 2} = 1/9, 2/9$, and the background contribution with $\mathcal{T}_g^{\Delta 2} = 1, 2/9$ is the most, or at least equally, important.

These cross terms contribute to the background and cannot be dressed by the Δ self-energy. The same kind of analysis can be done for the other $\frac{1}{2}$ resonances that have the same isospin factors that the direct and cross nucleon terms [Figs. 1(b) and 1(a)], but with a much lower contribution of these regards the Δ. This analysis is an indication that including rescattering effects could be more important that adding more and more energetic resonances, since background contributions will grow anyway. Summarizing, all background contributions coming from nonresonant origin plus cross-resonant terms [Figs. 1(a)–1(g)] cannot be dressed by a self-energy and its behavior could be corrected by taking into account the rescattering through T_{NP} as discussed in the previous subsection.

As was mentioned, in Eqs. (15) and (16) $\mathcal{O}^\lambda$ should be affected by a FF. To solve numerically the $\mathcal{P}$ integrals is not trivial, and we will assume the minimum approach of considering the following:

(1) The use of effective couplings in W^λ_{WNR}, that is $\tilde{W}^\lambda_{WNR} \to W^\lambda_{WNR}$ (effective weak couplings) to simulate the effect of the second term of Eq. (16), which was shown satisfactory for the case of photoproduction [28]. These effective values are the empirical ones adopted in our previous work [24]. Same will be valid for $\mathcal{O}^\lambda_B$ where weak empirical or experimental coupling constants are used.

(2) To avoid model dependencies coming from the introduction of arbitrary FF at each interaction vertex, we will introduce a global form factor (17) in the decay amplitude. The using of FF at each vertex requires the introduction of vertex corrections to keep for example electromagnetic gauge invariance. As we are including resonances with effects until around $W_{\pi N} \sim 1.6$ GeV, taking into account the width of the most energetic considered one [$S_{11}(1535)$ MeV], we will only light on this FF above this energy.

In this way, we also correct the amplitude for the excitation of more energetic resonances, which were not considered through the effective monopole form in Eq. (19) (see the following discussion), in our model since now we wish to describe data without $W_{\pi N}$ cuts. Guided by a previous proper description on NC1π data obtained by the CERN Gargamelle experiment without applying cuts in the neutrino energies [25], we multiply $\mathcal{O}_B^\lambda + \mathcal{O}_R^\lambda$ by a global regularizing FF of the $\Delta\pi N$ and $N\pi N'$ vertexes described above in Eq. (17). We adopt the value $\Lambda = 600$ MeV in consistency with Ref. [25]. Also we throw out the $\mathcal{P}$ contribution in the first bracket of Eq. (15) modify only the on shell potential as a first minimum modification to the model and that was appropriated when we discussed NC1π [25]. Summarizing, this FF should take into account the hadron structure and the possibility of exciting more energetic resonances when $W_{\pi N}$ grows in an effective fashion.

Now, we discuss with more detail the calculations with $W_{\pi N} \lesssim 2$ GeV and compare with data without cuts. As we have seen in the previous Fig. 2, the model used to treat the self-energy in the propagators leads to different results. First, we will use the CMS + CMW approaches that assume a constant width; second, we will keep the same propagators but with the energy dependent width in Eqs. (7) and (8); and finally we assume the exact Δ (that is, the main contributing one) propagator. In this last case, the self-energy changes the structure of the Δ propagator [36], but we assume the simplification of using the same effective mass and width of the CMS approach. Results are shown in the Fig. 3. As can be seen, the tendency of increasing the cross section by the second resonance region contribution is persistent as previously discussed [24], and the results that better reproduce globally the three channels of data is still the CMS + CMW approach with a constant width. When we enable an energy dependent width, we see a change that depends on the channel diminishing the results in the main one [Fig. 3(a)] and growing and diminishing in the other two [Figs. 3(b) and 3(c)]. When the exact propagator for the Δ is used, the results for the first channel are more diminished and an opposite effect is generated for the other two.

Nevertheless, an observation should be done in order. The parameters used for the Δ resonance ($f_{\pi N\Delta}$, m_Δ, Γ_Δ, G_E, G_M, D_1 or C_A^5) have been fitted using the CMS approach with a constant width, and thus if one wishes to use another approach, then a new fitting should be done. This could explain why the best fit is done with the simpler CMS approach, while the energy dependent width should not be a crucial change of parameters since we are keeping the same structure as the CMS propagator. In addition, as we are using a global FF that affects the full amplitude, and if the other resonances are treated within the CMW approach, then to use an exact propagator for the Δ would not be so consistent. Finally, it is evident that the FF taken from NC pion productions also work *s* very well here.

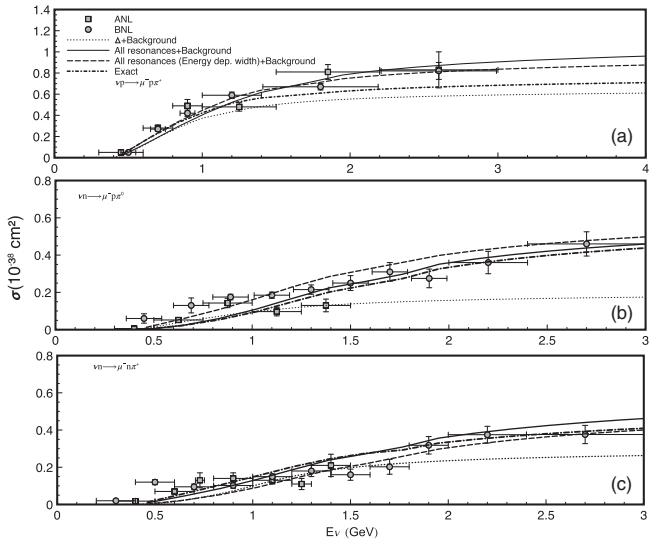

FIG. 3. Total νN cross section as function of the neutrino energy for different channels. Results with only the Δ and all resonances = Δ + second region's resonances, plus the corresponding background are shown for $W_{\pi N} \lesssim 2$ GeV. Data are taken from the reanalyzed ANL and BNL ones in Ref. [17]. Δ + background in CMS: dotted lines. All resonances + background in CMS + CMW: full lines. Same but with energy dependent width from Eqs. (7), (8): dashed lines. Finally, same but using the exact expression for the Δ propagator (see Ref. [36]): dashed-dotted lines

This is supported by the following analysis. As we have shown previously in Ref. [25], from where the parameter Λ in Eq. (19) was taken, the effect of the uncertainties in the parameters $D1(0)$ and M_A in the axial FF for the Δ resonance within the CMS model through a hatched area in Figs. 7 and 8 of [25]. There, it was shown that the uncertainty effects on the results is well below the data errors and the differences when we change from energy dependent to constant widths approaches. These two parameters were involved in the fitting we did on the flux averaged $d\sigma/dQ^2$ cross section in the previous Ref. [26] and then used in the following contributions, while the axial coupling for the another resonances were fixed from the Particle Data Group (PDG) values for masses and widths. As we are not doing any new fitting here but are using the parameters of previous works, we felt that it was not necessary to analyze the CMS + CMW parameter uncertainty effects again because they were under control.

As the fitting of the axial Δ parameters is achieved using the flux averaged differential cross section $\langle d\sigma/dQ^2\rangle$, we show the results for it within our model and compare it with the more recent ANL and BNL reanalyzed data [17]. In that reference results are shown for the events-Q^2 distribution in units of events/GeV^2 and as our results are given in 10^{-38} cm^2/GeV^2, we use the same conversion factor found in the total cross section calculation to compare with the data. They are reported without cuts and are compared with

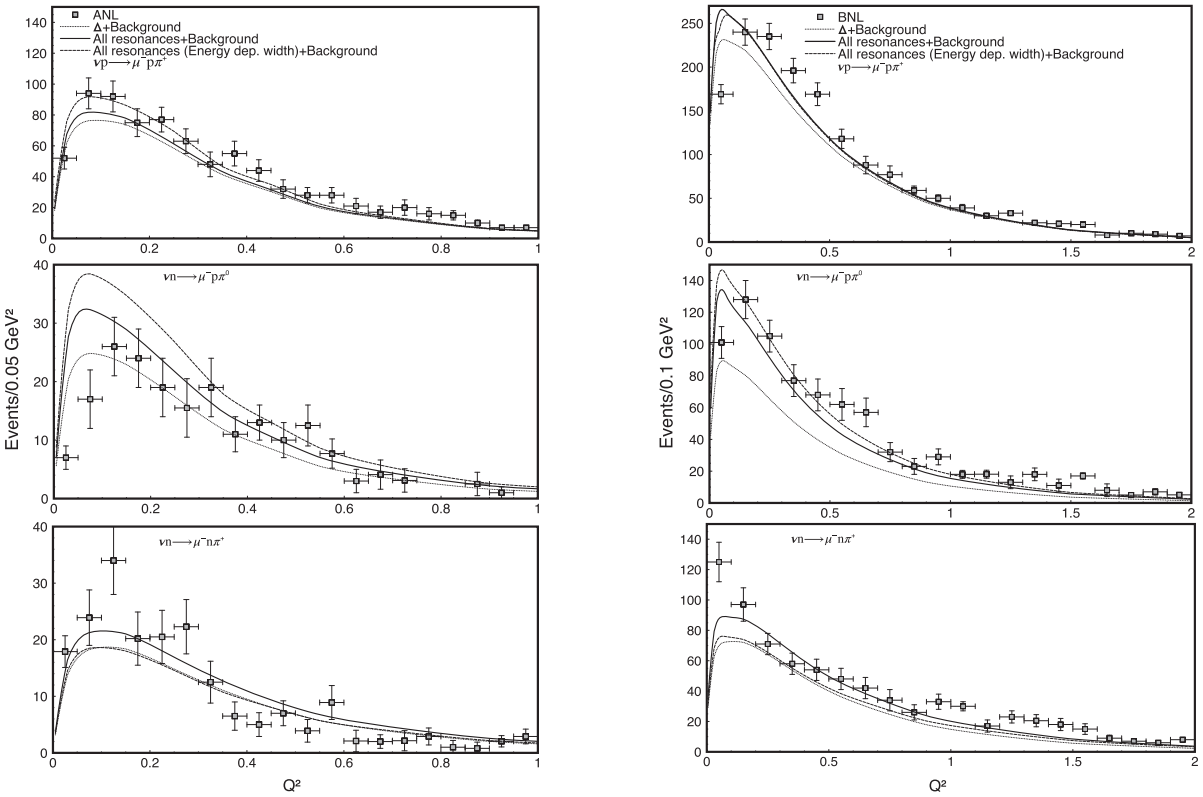

FIG. 4. Differential cross section with $W_{\pi N} \lesssim 2$ GeV. Line conventions are the same that in Fig. 3. Data are taken from Ref. [17].

our results in Fig. 4. We show calculations within the same approaches than the total cross section, but we avoid using the exact Δ propagator for the reasons exposed above. As can be seen, results within the constant width are acceptable in the three channels. We are not doing any new fit (the fixing of C_A^5 was done previously [30] using the ANL data with cuts $W_{\pi N} < 1.4$ GeV [6]), and the description is better that those done with GENIE in Ref. [17]. As can be seen, using the energy dependent width enlarges the first and second channels' theoretical results and diminishes those for the third one; this leads to a worse coincidence with data in an amount depending on the experiment (either ANL or BNL).

C. ANTINEUTRINOS

Now, in order to continue probing our model we wish to calculate the antineutrinos total cross section as was done in our previous work [24]. We have two differences regarding the neutrinos case. First, the interactions of neutrinos with hadrons are not the same as those for antineutrinos. We have a sign of difference in the lepton current contraction that makes a different coupling with the hadron one. Then, the interaction with neutrinos is different from antineutrinos due the use of spinors for antiparticles in the lepton current in Eq. (4) and has nothing to do with the very well-known CP violation. Second, in the experiment, an admixture of heavy freon CF3Br was exposed to the CERN PS antineutrino beam (peaked at $E_{\bar{\nu}} \sim 1.5$ GeV). In this case, the experiment informs us that we have 0.44% on neutrons and 0.55% of protons, and since our calculations were for free nucleons we weigh out results with these percentages depending on the channel. Our results include all resonances, and results for $W_{\pi N} \lesssim 2$ GeV are compared with the data reported in [38] and are shown in Fig. 5. As can be seen, we get a consistent description with that for the neutrino case. We show results within the CMS with only

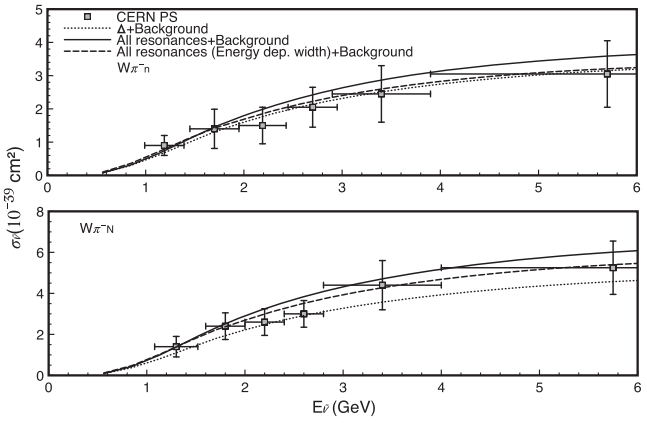

FIG. 5. Antineutrino's total cross sections with a $W_{\pi N} \lesssim 2$ GeV for the $\bar{\nu}n \to \mu^+ n\pi^-$ and that leads to a final $N\pi^-$ final state. Line conventions are the same that in Fig. 3.

the Δ and the Δ with the other resonances in the CMW, showing an appreciable difference between the different approaches. Adding the energy dependent width we get an improvement, but anyway we have consistence with the neutrino's results.

IV. CONCLUSIONS

We have extended our dynamical model to include resonances in the first and second regions, which were previously used to describe successful neutrino and antineutrino scattering cross sections of ANL data with the cuts $W_{\pi N} \lesssim 1.4$, 1.6 GeV, and to describe ANL and BNL data without cuts. The model consistently treats the vertexes and propagators for the spin-$\frac{3}{2}$ resonances from the point of view of contact transformations of the spin-$\frac{3}{2}$ Ψ_μ field and the role of the Ψ_0 component. In addition, we incorporate the different pole resonant contributions and background resonant and nonresonant ones in a coherently sum to the amplitude. We have added a global effective monopole FF to take into account the hadrons size and possible more energetic resonances excitations not included explicitly in the model for $W_{\pi N} \lesssim 2$. GeV. The data to compare are those that are reanalyzed to eliminate flux normalization uncertainties in the ANL and BNL experiments [16,17]. In the GENIE simulation used to describe the mentioned data [17], single pion production is separated into resonant and nonresonant terms, with interference between them neglected and interferences between resonances also neglected in the calculation. The resonant component is a modified version of the RS model [19], where the production and subsequent decay of 18 nucleon resonances with invariant masses $W \leq 2$ GeV are considered. In GENIE, only 16 resonances are included, based on the recommendation of the Particle Data Group [39]. In this work they make the assumption that interactions on deuterium can be treated as interactions on quasifree nucleons, which are only loosely bound together, and so neglect final state interaction effects. In GENIE, there are a number of systematic parameters that can be varied to change the single pion production model: resonant axial mass (M_A^{RES}), resonant normalization (RES norm), nonresonant normalization (DIS norm), and normalization of the axial form factor ($F_A(0)$). The total GENIE prediction is the incoherent sum of the RES and DIS contributions, where interference terms have been neglected. GENIE cannot describe all of the pion production channels well for the reanalyzed datasets. For example, the data of the $\nu_\mu n \to \mu^- p\pi^0$, $\nu_\mu n \to \mu^- n\pi^+$ channels are very similar, but there are large differences between the nominal GENIE predictions for these channels. The nonresonant component of the GENIE prediction, which contributes strongly to these channels, appears to be too large. Nevertheless, within our model these two channels are described properly. Finally, it can be seen from Fig. 3 of Ref. [17], where neutrino energy distribution is shown, that the nominal GENIE prediction fails to describe the low-Q^2 data well for some channels. We also note that the GENIE uncertainties are larger than the data suggests, and they may be reduced by tuning the GENIE model to the ANL and BNL data. The difference within our model of the low Q^2 distribution seems to be right. In addition, we describe the proper antineutrino cross section without cuts in the data. In conclusion, its seem that keeping control of the cross sections until the second resonance region ($W_{\pi N} \lesssim$ 1.6 GeV) enables a good description without cuts introducing the effect of finite size of hadrons and more energetic resonances in an effective way.

ACKNOWLEDGMENTS

A. M. acknowledges funding from CONICET and UNLP, and D. F. T. A. and D. E. J. A. from UdeA.

APPENDIX: BACKGROUND AND RESONANT AMPLITUDES

The background contributions to the amplitude read

$$
\begin{aligned}
&O_{\mathrm{B}}^{\lambda}(p,p',q) = O_{\mathrm{BN}}^{\lambda}(p,p',q) + O_{\mathrm{BR}}^{\lambda}(p,p',q),\\
&O_{\mathrm{BN}}^{\lambda}(p,p',q) = -i\frac{1}{2}\left[F_1^V(Q^2)\gamma^\lambda - i\frac{F_2^V(Q^2)}{2m_N}\sigma^{\lambda\nu}q_\nu - F^A(Q^2)\gamma^\lambda\gamma_5\right] i\frac{\not p' + \not q + m_N}{(p'+q)^2 - m_N}\frac{g_{\pi NN}}{2m_N}\gamma_5(\not p - \not p' - \not q)\sqrt{2}\mathcal{T}_a(m_t,m_{t'})\\
&\quad + \frac{g_{\pi NN}}{2m_N}\gamma_5(\not p - \not p' - \not q) i\frac{\not p - \not q + m_N}{(p-q)^2 - m_N^2}\left(-i\frac{1}{2}\right)\left[F_1^V(Q^2)\gamma^\lambda - i\frac{F_2^V(Q^2)}{2m_N}\sigma^{\lambda\nu}q_\nu - F^A(Q^2)\gamma^\lambda\gamma_5\right]\sqrt{2}\mathcal{T}_b(m_t,m_{t'})\\
&\quad - \frac{i}{(p-p')^2 - m_\pi^2} iF_1^V(Q^2)(2p - 2p' - q)^\lambda \times \frac{g_{\pi NN}}{2m_N}\gamma_5(\not p - \not p')\sqrt{2}\mathcal{T}_c(m_t,m_{t'}) + \frac{g_{\pi NN}}{2m_N}F_1^V(Q^2)\gamma_5\gamma^\lambda\sqrt{2}\mathcal{T}_d(m_t,m_{t'})\\
&\quad + i\frac{g_{\omega\pi V}}{m_\pi}F_1^V(Q^2)\epsilon^{\lambda\alpha\beta\delta}q_\alpha(p-p')_\beta i\frac{-g_{\delta\epsilon}}{(p-p')^2 - m_\omega^2}(-i)\frac{g_{\omega NN}}{2}\left[\gamma^\epsilon - i\frac{\kappa_\omega}{2m_N}\sigma^{\epsilon\kappa}(p-p')_\kappa\right]\sqrt{2}\mathcal{T}_e(m_t,m_{t'})\\
&\quad + f_{\rho\pi A}F^A(Q^2) i\frac{-g^{\lambda\mu}}{(p-p')^2 - m_\rho^2}(-i)\frac{g_{\rho NN}}{2}\left[\gamma_\mu - i\frac{\kappa_\rho}{2m_N}\sigma_{\mu\kappa}(p-p')^\kappa\right]\sqrt{2}\mathcal{T}_f(m_t,m_{t'}),
\end{aligned}
\tag{A1}
$$

$$
\begin{aligned}
O^{\lambda}_{\mathrm{BR}}(p,p',q) = & -i\frac{1}{2}\left[\frac{g^{1440}_{1V}}{(m_{1440}+m_N)^2}(Q^2\gamma^\lambda + \not{q}q^\lambda) - \frac{g^{1440}_{2V}}{(m_{1440}+m_N)}i\sigma^{\lambda\nu}q_\nu - g^{1440}_{1A}\gamma^\lambda\gamma_5 + \frac{g^{1440}_{3A}}{m_N}q^\lambda\gamma_5\right] \\
& \times i\frac{\not{p}'+\not{q}+m_R}{(p'+q)^2 - m^2_{1440} + i\Gamma_{1440}m_{1440}}(-)\frac{f_{1440\pi N}}{m_\pi}\gamma_5(\not{p}-\not{p}'-\not{q})\sqrt{2}\mathcal{T}^{1440}_g(m_t,m_{t'}) \\
& - i\frac{1}{2}\gamma_5\left[\frac{g^{1535}_{1V}}{(m_{1535}+m_N)^2}(Q^2\gamma^\lambda + \not{q}q^\lambda) - \frac{g^{1535}_{2V}}{(m_{1535}+m_N)}i\sigma^{\lambda\nu}q_\nu - g^{1535}_{1A}\gamma^\lambda\gamma_5 + \frac{g^{1535}_{3A}}{m_N}q^\lambda\gamma_5\right] \\
& \times i\frac{\not{p}'+\not{q}+m_{1535}}{(p'+q)^2 - m^2_{1535} + i\Gamma_{1535}m_{1535}}(-)\frac{f_{1535\pi N}}{m_\pi}(\not{p}-\not{p}'-\not{q})\sqrt{2}\mathcal{T}^{1535}_g(m_t,m_{t'}) \\
& + (-)\overline{W^{WN\Delta}_{\lambda\alpha}(p,p',-q)}iG^{\alpha\beta}_{\Delta}(p'+q)(-)\frac{f_{\Delta\pi N}}{m_\pi}(p-p'-q)_\beta\sqrt{2}\mathcal{T}^{\Delta}_g(m_t,m_{t'}) \\
& + (-)\overline{\frac{1}{2}W^{WN1520}_{\lambda\alpha}(p,p',-q)}iG^{\alpha\beta}_{1520}(p'+q)(-)\frac{f_{1520\pi N}}{m_\pi}\gamma_5(p-p'-q)_\beta\sqrt{2}\mathcal{T}^{1520}_g(m_t,m_{t'}),
\end{aligned}
\tag{A2}
$$

where $\frac{1}{2}$ resonances are put before the $\frac{3}{2}$ ones. $G^{\alpha\beta}_R$ together with $W^{WNR} = (V^{WNR} + A^{WNR})$ are the spin-$\frac{3}{2}$ resonance propagators and $WN \to R$ vertexes, respectively, both defined in Ref. [24] while $\bar{W} = \gamma_0 W^\dagger \gamma_0$. V^{WNR} is the vector vertex as in the pion-photo ($Q^2 = 0$) [28] and the electroproduction applying conserved Vector current (CVC) within the Sachs parametrization, and A^{WNR} is the axial contribution compatible with $V^{WN\Delta}_{\nu\mu}$ [26] (it could be, in principle, obtained by using $-V^{WN\Delta}_{\nu\mu}\gamma_5$).

The corresponding pole contributions coming from the resonances are

$$
\begin{aligned}
\mathcal{O}^{\lambda}_R = & \frac{f_{1440\pi N}}{m_\pi}\gamma_5(\not{p}-\not{p}'-\not{q})i\frac{\not{p}-\not{q}+m_R}{(p-q)^2 - m^2_{1440} + i\Gamma_{1440}m_{1440}} \\
& \times (-i)\frac{1}{2}\left[\frac{g^{1440}_{1V}}{(m_{1440}+m_N)^2}(Q^2\gamma^\lambda + \not{q}q^\lambda) - \frac{g^{1440}_{2V}}{(m_{1440}+m_N)}i\sigma^{\lambda\nu}q_\nu - g^{1440}_{1A}\gamma^\lambda\gamma_5 + \frac{g^{1440}_{3A}}{m_N}q^\lambda\gamma_5\right]\sqrt{2}\mathcal{T}^{1440}_h(m_t,m_{t'}) \\
& + (-)\frac{f_{1535\pi N}}{m_\pi}(\not{p}-\not{p}'-\not{q})i\frac{\not{p}-\not{q}+m_{1535}}{(p-q)^2 - m^2_{1535} + i\Gamma_{1535}m_{1535}} \\
& \times (-i)\frac{1}{2}\left[\frac{g^{1535}_{1V}}{(m_{1535}+m_N)^2}(Q^2\gamma^\lambda + \not{q}q^\lambda) - \frac{g^{1535}_{2V}}{(m_{1535}+m_N)}i\sigma^{\lambda\nu}q_\nu - g^{1535}_{1A}\gamma^\lambda\gamma_5 + \frac{g^{1535}_{3A}}{m_N}q^\lambda\gamma_5\right]\gamma_5\mathcal{T}^{1335}_h(m_t,m_{t'}) \\
& + (-)\frac{f_{\Delta\pi N}}{m_\pi}(p-p'-q)_\alpha iG^{\alpha\beta}_{\Delta}(p-q)W^{WN\Delta}_{\beta\lambda}(p,p',q)\sqrt{2}\mathcal{T}^{\Delta}_g(m_t,m_{t'}) \\
& + (-)\frac{f_{1520\pi N}}{m_\pi}\gamma_5(p-p'-q)_\alpha iG^{\alpha\beta}_{\Delta}(p-q)W^{WN1520}_{\beta\lambda}(p,p',q)\sqrt{2}\mathcal{T}^{1520}_g(m_t,m_{t'}),
\end{aligned}
\tag{A3}
$$

where all the vector and axial weak FF present in Eqs. (A1)–(A3) are defined in Ref. [24]. Note that the $\frac{1}{2}$ factor in the weak vertex of the spin-$\frac{1}{2}$ resonances comes from the isovector part of the charge operator $\frac{\tau_3}{2}$ dragged from the CVC hypothesis.

[1] 1. B. Eberly *et al.*, Phys. Rev. D **92**, 092008 (2015).
[2] T. Le *et al.*, Phys. Lett. B **749**, 130 (2015).
[3] A. Aguilar-Arevalo *et al.*, Phys. Rev. D **83**, 052007 (2011).
[4] J. T. Sobczyk and J. Żmuda, Phys. Rev. C **91**, 045501 (2015).
[5] 5. U. Mosel, Phys. Rev. C **91**, 065501 (2015).
[6] G. M. Radecky *et al.*, Phys. Rev. D **25**, 1161 (1982).
[7] T. Kitagaki *et al.*, Phys. Rev. D **34**, 2554 (1986).
[8] E. Hernandez, J. Nieves, and M. Valverde, Phys. Rev. D **76**, 033005 (2007).
[9] T. Leitner, O. Buss, L. Alvarez-Ruso, and U. Mosel, Phys. Rev. C **79**, 034601 (2009).
[10] E. Hernandez, J. Nieves, M. Valverde, and M. Vicente Vacas, Phys. Rev. D **81**, 085046 (2010).
[11] M. Ahn *et al.*, Phys. Rev. Lett. **90**, 041801 (2003).
[12] K. Abe *et al.*, Phys. Rev. D **88**, 032002 (2013).
[13] O. Lalakulich and U. Mosel, Phys. Rev. C **87**, 014602 (2013).
[14] K. Graczyk, D. Kielczewska, P. Przewlocki, and J. Sobczyk, Phys. Rev. D **80**, 093001 (2009).

[15] K. M. Graczyk, J. Zmuda, and J. T. Sobczyk, Phys. Rev. D **90**, 093001 (2014).
[16] C. Wilkinson, P. Rodrigues, S. Cartwright, L. Thompson, and K. McFarland, Phys. Rev. D **90**, 112017 (2014).
[17] Philip Rodrigues, Callum Wilkinson, and Kevin McFarland, Eur. Phys. J. C **76**, 474 (2016).
[18] C. Andreopoulos, A. Bell, D. Bhattacharya, F. Cavanna, J. Dobson *et al.*, Nucl. Instrum. Methods Phys. Res., Sect. A **614**, 87 (2010).
[19] D. Rein and L. M. Sehgal, Ann. Phys. (N.Y.) **133**, 79 (1981).
[20] P. Adamson *et al.* (NOvA Collaboration), Phys. Rev. D **93**, 051104 (2016).
[21] M. Kirchbach and D. Ahluwalia, Phys. Lett. B **529**, 124 (2002).
[22] D. Badagnani, A. Mariano, and C. Barbero, J. Phys. G **39**, 035005 (2012).
[23] D. Badagnani, A. Mariano, and C. Barbero, J. Phys. G **44**, 025001 (2017).
[24] D. F. Tamayo Agudelo, A. Mariano, and D. E. Jaramillo Arango, companion paper, Phys. Rev. D **105**, 033008 (2022).
[25] A. Mariano, C. Barbero, and G. López Castro, Nucl. Phys. **A849**, 218 (2011).
[26] C. Barbero, A. Mariano, and G. Lopez Castro, Phys. Lett. B **664**, 70 (2008).
[27] C. Barbero and A. Mariano, J. Phys. G **42**, 105104 (2015).
[28] A. Mariano, Phys. Lett. B **647**, 253 (2007); J. Phys. G **34**, 1627 (2007).
[29] M. el Amiri, J. Pestieau, and G. López Castro, Nucl. Phys. **A543**, 673 (1992).
[30] G. Lopez Castro and A. Mariano, Nucl. Phys. **A697**, 440 (2002).
[31] T. Melde, L. Canton, and W. Plessas, Phys. Rev. Lett. **102**, 132002 (2009).
[32] T. Feuster and U. Mosel, Phys. Rev. C **58**, 457 (1998); T. Sato and T.-S. H. Lee, Phys. Rev. C **54**, 2660 (1996).
[33] T. Sato and T.-S. H. Lee, Phys. Rev. C **54**, 2660 (1996).
[34] B. C. Pearce and B. K. Jennings, Nucl. Phys. **A528**, 655 (1991).
[35] At first, it is possible to manipulate the FF proposed in those references to get forms very similar to Eq. (17).
[36] C. Barbero, A. Mariano, and G. Lopez Castro, Phys. Lett. B **728**, 282 (2014).
[37] O. Lalakulich, E. A. Paschos, and G. Piranishvili, Phys. Rev. D **74**, 014009 (2006).
[38] T. Bolognese, J. P. Engel, J. L. Guyonnet, and J. L. Riester, Phys. Lett. **81B**, 393 (1979).
[39] W.-M. Yao *et al.*, J. Phys. G **33**, 1 (2006).